MCB
Journals.ASM.org

Dynamic Loss of H2B Ubiquitylation without Corresponding Changes in H3K4 Trimethylation during Myogenic Differentiation

Vasupradha Vethantham,[a] Yan Yang,[a] Christopher Bowman,[a] Patrik Asp,[a]* Jeong-Heon Lee,[b] David G. Skalnik,[c] and Brian D. Dynlacht[a]

Department of Pathology and Cancer Institute, Smilow Research Center, New York University School of Medicine, New York, New York, USA[a]; Herman B. Wells Center for Pediatric Research, Section of Pediatric Hematology/Oncology, Indiana University School of Medicine, Indianapolis, Indiana, USA[b]; and Biology Department, School of Science, Indiana University Purdue University, Indianapolis, Indiana, USA[c]

Ubiquitylation of H2B on lysine 120 (H2Bub) is associated with active transcriptional elongation. H2Bub has been implicated in histone cross talk and is generally regarded to be a prerequisite for trimethylation of histone 3 lysine 4 (H3K4me3) and H3K79 in both yeast and mammalian cells. We performed a genome-wide analysis of epigenetic marks during muscle differentiation, and strikingly, we observed a near-complete loss of H2Bub in the differentiated state. We examined the basis for global loss of this mark and found that the H2B ubiquitin E3 ligase, RNF20, was depleted from chromatin in differentiated myotubes, indicating that recruitment of this protein to genes substantially decreases upon differentiation. Remarkably, during the course of myogenic differentiation, we observed retention and acquisition of H3K4 trimethylation on a large number of genes in the absence of detectable H2Bub. The Set1 H3K4 trimethylase complex was efficiently recruited to a subset of genes in myotubes in the absence of detectable H2Bub, accounting in part for H3K4 trimethylation in myotubes. Our studies suggest that H3K4me3 deposition in the absence of detectable H2Bub in myotubes is mediated via Set1 and, perhaps, MLL complexes, whose recruitment does not require H2Bub. Thus, muscle cells represent a novel setting in which to explore mechanisms that regulate histone cross talk.

Modifications of histones, including lysine methylation, acetylation, and ubiquitylation, are closely associated with the control and modulation of gene transcription. Chromatin modifications are often asymmetrically deposited with respect to transcription start sites (TSS) of genes. In mammalian cells, lysine 4 trimethylation of histone H3 (H3K4me3) is associated with the TSS and 5′ ends of genes, whereas H2B monoubiquitylation at lysine 120 (H2Bub) and H3K36 trimethylation are associated with transcribed regions of genes (22). H2Bub is catalyzed by a heterodimeric E3 ubiquitin ligase complex comprised of RNF20 and RNF40 (Bre1a/b in yeast) (11, 46) and the E2 ubiquitin-conjugating enzyme, Rad6 (12, 13, 30). H2Bub has been associated with active transcription and, more specifically, with transcriptional elongation (43). Several groups have independently demonstrated that H2Bub is a prerequisite for H3K79 and H3K4 methylation in yeast through a transtail mechanism (6, 8, 24, 37). While monomethylation of H3K4 and H3K79 was found to be H2Bub independent (7, 33), H2Bub has been shown to direct di- and trimethylation of H3K4 and H3K79 through the recruitment of relevant enzymes, Set1 and Dot1, respectively, facilitating histone cross talk in both yeast and mammals (12, 19, 37).

The PAF1 complex (Paf1C) has also been shown to play a role in the regulation of H2B ubiquitylation in both yeast and mammals via recruitment and activation of Rad6/RNF20 on transcribed regions of chromatin in a manner that is dependent on elongating RNA polymerase (24, 43, 46). In addition, the Bur1 kinase in yeast and CDK9 in humans were shown to promote deposition of H2Bub (15, 29). Thus, H2B monoubiquitylation is closely linked to transcriptional elongation. However, H2Bub is not simply a by-product of elongation, since it has been shown to play an active role in promoting efficient transcription elongation. In this context, H2Bub is thought to regulate transcriptional elongation through the FACT complex, a histone H2A/H2B chaperone known to destabilize nucleosomes (26, 32), which could in turn regulate H2Bub deposition. Reciprocally, H2Bub could also facilitate FACT function by modulating chromatin dynamics during transcriptional elongation (10, 28), since recent structural studies have shown that H2Bub interferes with chromatin compaction, promoting a more "open" chromatin conformation, thus facilitating transcription (9). Depletion of H2Bub in mammalian cells alters the expression of a subset of ubiquitylated genes (35). In yeast, H2Bub seems to play a broader role in gene expression above and beyond its functions in histone cross talk, since abrogating H2Bub results in growth defects and changes in gene expression that are more severe than those observed upon abolishing H3 methylation alone (38). More recently, H2Bub was shown to modulate nucleosome dynamics and gene expression in yeast in a manner unrelated to its aforementioned role in histone cross talk, through regulation of both transcriptional initiation and elongation (4). In contrast with the *in vitro* study (9), H2Bub was shown to have a stabilizing effect on nucleosome assembly *in vivo*, in a manner that was largely independent of transcription (4).

While the role of H2Bub has been thoroughly explored in yeast, many questions remain regarding the functional role of this modification in mammalian cells. In particular, the role of this modification in cell type specification, if any, remains unknown.

Received 28 July 2011 Returned for modification 17 August 2011
Accepted 5 January 2012
Published ahead of print 17 January 2012
Address correspondence to Brian D. Dynlacht, brian.dynlacht@med.nyu.edu.
* Present address: Liver Transplant Program, Montefiore Medical Center, Albert Einstein College of Medicine, Bronx, New York, U.S.A.
Y.Y. and C.B. contributed equally to this article.

doi:10.1128/MCB.06026-11

In this study, we have investigated the genome-wide role of H2Bub during skeletal myogenesis using a combination of chromatin immunoprecipitation and sequencing (ChIP-seq) and expression profiling, allowing us to make several surprising observations regarding this modification in muscle cells. We observed a striking and global depletion of H2Bub during myogenic differentiation, and this loss was not associated with changes in gene expression. Remarkably, the overall depletion of H2Bub did not lead to diminished H3K4 methylation, suggesting an unexpected dissociation of these modifications in differentiated myotubes (MT). The results of mechanistic studies indicated that the global loss of H2Bub in differentiated cells was due, at least in part, to reduced recruitment of RNF20. Wdr82 is a component of the COMPASS/Set1 complex known to recruit this H3K4 methyltransferase to chromatin in an H2Bub-dependent manner in yeast and mammalian cells. Nevertheless, we show that in myotubes, COMPASS/Set1 was efficiently recruited to multiple genes despite the absence of detectable H2Bub. Thus, muscle cells display unique and dynamic changes in H2B ubiquitylation and unexpected variations in the mechanisms that link this mark with H3K4 methylation.

MATERIALS AND METHODS

Cell culture. The C2C12 murine myoblast cell line was obtained from Sigma and cultured as described previously (5). Briefly, cells were cultured in Dulbecco's modified Eagle's medium (DMEM) supplemented with 10% fetal bovine serum (FBS). Differentiation was induced by growing cells to confluence and supplementing the medium with 2% horse serum. After 4 days in differentiation medium, differentiated myotubes were separated from undifferentiated cells with diluted trypsin. Primary human myoblasts were obtained from Lonza and cultured according to the manufacturer's instructions.

Preparation of chromatin and ChIP. Cells were cross-linked, harvested, and lysed as described previously (5), and sonication was performed to obtain fragments of 350 bp. Mononucleosomes were prepared as detailed previously (39). For ChIP-seq, titrations with various amounts of chromatin and antibodies were carried out, and ChIP assays were optimized to ensure antibody excess. Quantitative ChIP (qChIP) was performed as previously described (5). Unless otherwise indicated in the figure legends, all ChIP experiments were performed in triplicate and error bars used to denote standard errors of the means (SEM). The antibodies used for ChIP were monoubiquitinated histone H2B (Millipore 05-312), histone H2B (Abcam ab-1790), histone H3-trimethyl K4 (Abcam ab-8850; Active Motif catalog no. 36159), RNF20 (Abcam ab-32629) Paf1 and FACT (gift from D. Reinberg), Set1A, Cfp1, and Wdr82 (17), Menin (Bethyl A300-105A), and H3K79me3 (Abcam ab-2621).

ChIP-seq. The preparation of ChIP DNA libraries for sequencing was detailed previously (3). Libraries were sequenced using an Illumina GAII at the NYU genome sequencing facility using 6 picomoles of library per sample. Data analysis using the Qeseq peak-finding program, processing, and filtering procedures has been described previously (3).

RT-PCR and quantitative real-time PCR. RNA isolation and reverse transcription were performed as described in Acosta-Alvear et al. (1). Real-time quantitative PCR after ChIP and reverse transcription were performed as described previously (3). For qChIP-PCR, the amplicons were between 80 and 150 bp long, and the median position of each amplicon is denoted beside the gene within parentheses in the figures.

RNAi experiments. Small interfering RNA (siRNA) transfections were carried out in growing myoblasts with specific siRNAs targeting genes of interest and nonspecific controls (Dharmacon) using siImporter (Millipore) according to the manufacturer's protocol. For ChIP experiments, myoblasts were cross-linked and harvested 48 to 72 h after transfection. Sonicated chromatin was prepared as described previously (5). RNA interference (RNAi) experiments were performed 3 to 6 times. Construction of retroviral vectors expressing miRNAs, packaging of viral particles, and infections were carried out as described earlier (2). The siRNA and microRNA (miRNA) sequences targeting RNF20 were, respectively, GAGATTCTGTTAAGGATAA and GCATCATCCTTAAACGTTA. The Wdr82-targeting siRNA sequence was AGAGAACCCTGTACAGTAA.

Enrichment of chromatin. A standard CsCl purification method was employed as described previously (25, 27). Briefly, crude chromatin prepared as detailed above was layered onto a CsCl gradient and subjected to ultracentrifugation at 40,000 $\times$ *g* for 20 h. Chromatin-containing fractions from the gradient were analyzed by agarose gel electrophoresis, dialyzed, and frozen in aliquots at −80°C. Cross-links in purified chromatin were reversed by boiling in Laemmli buffer, and proteins were subjected to Western analyses. Nuclei were partitioned into soluble (S3) and chromatin (P3) fractions as described previously (21).

Microarray data accession number. All ChIP-seq data have been deposited in the Gene Expression Omnibus under GEO accession number GSE34960.

RESULTS AND DISCUSSION

H2B ubiquitylation is essentially erased during myogenic differentiation. We took advantage of the well-established mouse C2C12 model for muscle differentiation. C2C12 myoblasts proliferate rapidly in the presence of growth factors, and they readily differentiate into myotubes after mitogen depletion. We analyzed global changes in histone modifications associated with muscle differentiation (3), and during the course of this investigation, we observed a striking, near-complete loss of H2Bub from the chromatin fraction in myotubes by Western analyses (Fig. 1A). More detailed kinetic analyses indicated that H2Bub was robust in myoblasts and persisted in cells that had attained confluence and had begun exiting the cell cycle (time zero [T_0]) but was extinguished early in differentiation (within 24 h after induction of differentiation [T_{24}]) (Fig. 1B). Further, we examined whether these findings pertained to human cells by performing Western blot analyses on primary human myoblasts and differentiated myotubes. These results mirrored our findings in mouse C2C12 cells, indicating that the loss of H2Bub during myogenic differentiation occurs in both mouse and human cells (Fig. 1C).

We combined chromatin immunoprecipitation (ChIP) with massively parallel sequencing (ChIP-seq) to identify regions marked with H2Bub in growing C2C12 myoblasts (GM) and fully differentiated myotubes (MT) (3). Our ChIP-seq analysis of myoblast chromatin showed that H2Bub was extensively enriched within coding regions of genes, in accordance with previously published work (22) (Fig. 1D). Remarkably, myotubes exhibited pervasive and near-complete loss of H2Bub. By merging our ChIP-seq data with expression profiles of myoblasts and myotubes (3), we showed that (i) H2Bub strongly correlated with gene expression and (ii) the mark was primarily found on actively transcribed genes in myoblasts (Fig. 1D). Interestingly, the highest levels of H2Bub were found on moderately and highly expressed genes, as previously reported (22, 34). In contrast, genes that were never expressed lacked this mark in both states (Fig. 1E). We also plotted H2Bub enrichment on genes grouped according to dynamic changes in expression during myogenic differentiation (3), and on a population level, we observed dramatic downregulation of H2Bub in myotubes, consistent with our Western blot data. The loss of H2Bub did not coincide with changes in gene expression in MT, and indeed, this mark was strikingly absent from

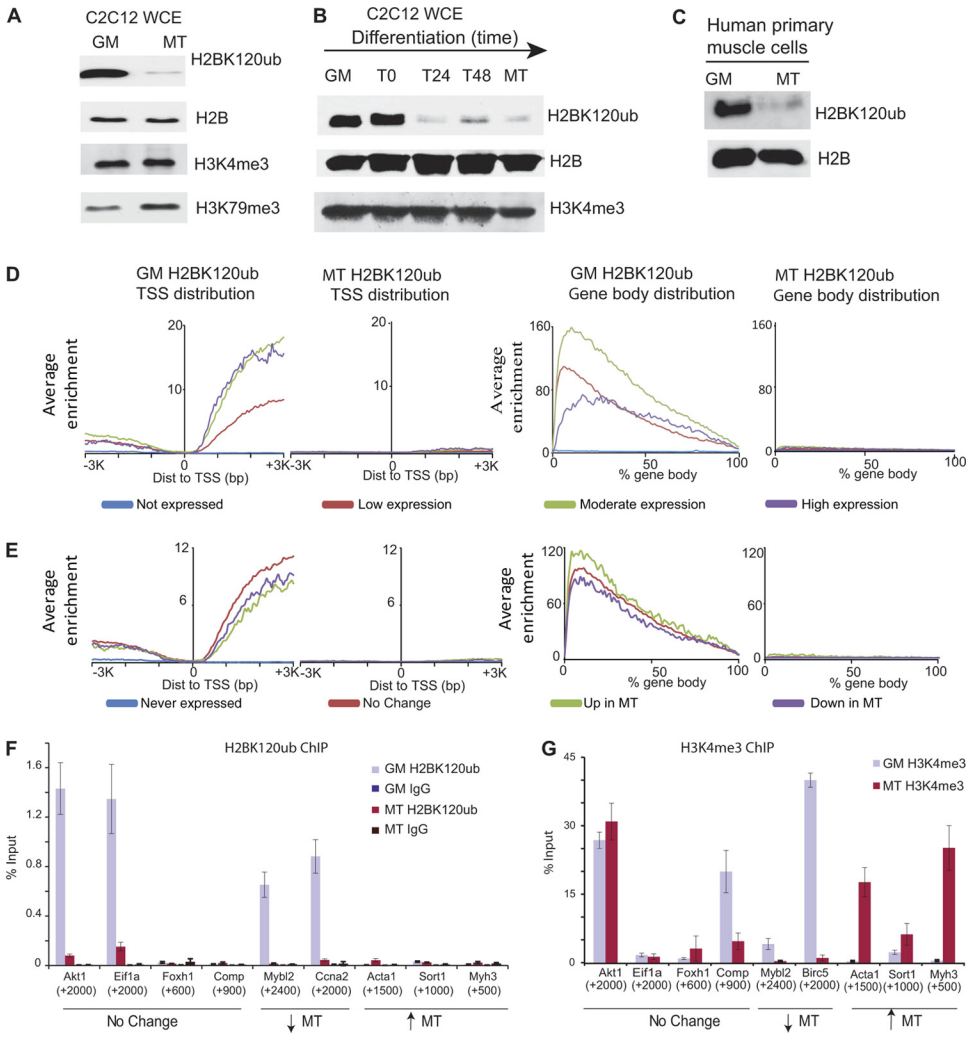

FIG 1 Global loss of H2Bub (H2BK120ub; H2B monoubiquitylated on lysine 120) during myogenic differentiation. (A and C) Western blots show diminution of H2Bub and changes in H3K4me3 during myogenic differentiation. Cell extracts from the indicated populations of C2C12 (A) or primary human growing myoblasts (GM) or myotubes (MT) (C), as indicated, were probed with the antibodies shown at right. (B) Myogenic differentiation time course. Lysates of cells prior to induction of differentiation (T0) and those corresponding to the indicated number of hours after induction (24 or 48 h, T24 and T48, respectively) were probed. (D and E) Genome-wide analysis of H2Bub in growing myoblasts and myotubes. Distribution of H2Bub on the indicated sets of genes, grouped and color coded according to absolute (D) or relative (E) expression levels during differentiation. Average enrichment is shown on the *y* axis, and plots show enrichment with respect to TSS (left) or gene body (right) distributions. Dist, distance. (F and G) qChIP was carried out using the H2Bub antibody (F) or H3K4me3 antibody (G) in growing myoblasts and differentiated myotubes. Enrichment with a nonspecific control antibody (IgG) is shown. Percent input is indicated on the *y* axis. The median position of each gene amplicon is depicted in parentheses. The expression groups of the genes are indicated below the graphs.

groups of genes that were highly expressed and/or upregulated in myotubes (Fig. 1D and E).

We used quantitative ChIP (qChIP) with primers amplifying transcribed regions of genes to confirm that H2Bub was present on actively transcribed genes in myoblasts, irrespective of their expression state in myotubes (i.e., either constitutively expressed or downregulated genes) (Fig. 1F and data not shown). In every case, we confirmed that these genes dramatically lost H2Bub in myotubes. Remarkably, when we examined genes that are markedly upregulated in MT, we found that each of the genes (e.g., *Acta1*, *Sort1*, *Trim63*, and *Myh3*) displayed very low or undetectable levels of H2Bub in either condition (Fig. 1F). Thus, it appears that gene expression and H2Bub deposition are not tightly associated in fully differentiated myotubes, unlike myoblasts where H2Bub positively correlates with gene expression.

Our ChIP-seq experiments identified relatively few genes with robust levels of H2Bub in myotubes, and even fewer genes showed enrichment for this mark in myotubes without prior deposition of this modification in myoblasts. Indeed, we confirmed that H2Bub was found on a subset of these genes in myotubes by qChIP and found few instances in which the mark appeared in myotubes only (data not shown). This suggests that *de novo* ubiquitylation of H2B may be disfavored in myotubes, although it may be maintained on a few genes that are highly expressed in that condition.

Myotubes exhibit retention and acquisition of H3K4me3 despite dramatic downregulation of H2Bub. Acquisition of di- and trimethylated H3K4 has been shown to depend on H2Bub deposition both in yeast and mammalian cells (8, 12, 37). Therefore, the global loss of H2Bub from myotube chromatin, reflected in our Western analysis and ChIP-seq experiments (Fig. 1A), was

surprising. Strikingly, total levels of H3K4me3 were similar in both conditions despite the near-complete loss of H2Bub, both on Western blots and in our ChIP-seq data reported previously (Fig. 1A and B) (3). As reported earlier (22, 35), while H3K4me3 and H2Bub signals overlapped in regions downstream of the TSS, H2Bub enrichment extends further into the gene body, indicative of its roles in elongation and nucleosome dynamics. In our studies, we have focused on H3K4me3 enrichment downstream of the TSS rather than promoter methylation, as only the former was found to be correlated with H2Bub enrichment in mammalian cells (22).

To further examine potential cross talk between histone modifications, we analyzed our ChIP-seq data as nonquantitative high-density maps (HDMs) of histone marks over regions spanning from 3 kb upstream to 9 kb downstream of the TSS (3). We focused our attention on genes that were upregulated in myotubes or that were constitutively expressed in both conditions, since both groups would be expected to show significant levels of H3K4me3 at one or both stages (Fig. 2A and B). Our HDMs identified a group of genes upregulated in myotubes that displayed robust H3K4 trimethylation in both myoblasts and myotubes, although H2B ubiquitylation was restricted to myoblasts (Fig. 2A). In addition, we observed a group of genes that were never ubiquitylated on H2B but that were nevertheless strongly upregulated in MT, concomitant with a robust increase in H3K4me3 (Fig. 2A). Further, the constitutively expressed group (which exhibited little or no change in expression during differentiation) retained high levels of H3K4me3 in myotubes despite the near complete loss of H2Bub. Interestingly, a subset of genes had no detectable H2Bub in myoblasts although they displayed robust H3K4me3. Importantly, we used qChIP to confirm our genome-wide analyses by designing primers to amplify regions downstream of the TSS that exhibited overlap between the two marks in ChIP-seq, and we detected significant levels of H3K4me3 on genes in myotubes that were constitutively expressed or upregulated in that condition despite the absence of H2Bub (Fig. 1F and G).

These experiments did not address the possibility that H2Bub might be transiently deposited on nucleosomes prior to differentiation, and since cells that have exited the cell cycle no longer undergo histone replacement as a result of DNA replication, the more stable H3K4me2/3 modification could persist on nucleosomes even in the absence of H2Bub. In this setting, continuous H2B ubiquitylation would not be needed to maintain H3K4me3 levels. To address this possibility, we performed qChIP on genes during a differentiation time course (Fig. 2C). As cells exited the cell cycle (T_0), H2Bub levels declined precipitously on genes that were expressed constitutively or downregulated in myotubes, and within 24 h after differentiation (T_{24}), most genes exhibited background levels of H2Bub. However, H2Bub was not detected at any time point on genes upregulated in myotubes (Fig. 2C).

On genes that were downregulated in myotubes (e.g., *Suv39h1* and *Mybl2*), H3K4me3 and H2Bub levels declined in parallel. In contrast, the H3K4me3 profiles on genes that were upregulated or constitutively expressed differed dramatically from those of H2Bub (Fig. 2C). Constitutively expressed genes retained significant levels of H3K4me3 despite losing the H2Bub mark (e.g., *Akt1*) or exhibited robust levels of H3K4me3 in either condition despite the presence of background levels of H2Bub (e.g., *Comp*), as observed in our HDMs. Upregulated genes, on the other hand, exhibited significant increases in H3K4me3 (generally at T_{24}), concomitant with gene activation, despite negligible (background) levels of H2Bub at all stages of the differentiation time course (e.g., *Sort1*, *Acta1*, and *Trim63*). Since our experiments were performed under steady-state conditions, highly dynamic changes in H2Bub could not be measured on these genes, and therefore, we cannot rule out the possibility of rapid turnover of H2Bub, which could promote the acquisition of H3K4me3 in myotubes. In addition, our observations cannot rule out compensatory mechanisms, which could restore H3K4me3 after loss of H2Bub on constitutively expressed genes (such as *Akt1*). Nevertheless, it is striking that robust H3K4 trimethylation can be detected on a large number of genes in myotubes despite the presence of negligible levels of H2Bub (Fig. 2A). Our observations demonstrate an unexpected divergence between the levels of these two chromatin marks, and this effect is most prominent in the differentiated state.

Previous studies have also indicated that H3K79me3 and H2Bub are tightly coupled in yeast and mammalian cells, and H2Bub deposition is thought to be essential for the activity of the H3K79 methyltransferase, Dot1 (19, 20). Furthermore, studies in yeast suggest links between H3K4 and H3K79 methylation through incompletely defined mechanisms (19, 24, 37). Therefore, we performed qChIP to detect H3K79me3 on a subset of genes with diverse levels of H2Bub (Fig. 2C). Interestingly, unlike H3K4me3, we found that H3K79me3 levels, in general, paralleled those of H2Bub. For example, when H2Bub levels were low or negligible, H3K79 trimethylation was correspondingly very low on several genes (*Comp*, *Sort1*, and *Trim63*). In addition, we found that, for several genes (e.g., *Akt1*, *Suv39h1*, and *Mybl2*), the kinetics of H3K79me3 and H2Bub deposition paralleled one another during differentiation (Fig. 2C). These findings strongly suggest that genes can be trimethylated on H3K4 during myogenic differentiation without an obligatory link to H2Bub and H3K79me3.

Chromatin modifications on genes encoding MRFs. Given the pivotal role of muscle regulatory factors (MRFs) in myogenesis, we investigated chromatin modifications associated with each gene (*MyoD1*, *Myf5*, *Myf6*, and *Myog*) (Fig. 2D). *MyoD1* and *Myf6* are expressed in myoblasts and throughout differentiation, *Myf5* is expressed in myoblasts and early in differentiation, and *Myog* is most highly expressed during mid-late differentiation. Consistent with these expression data, *MyoD1*, *Myf5*, and *Myf6* exhibited robust H3K4me3 in myoblasts and myotubes, whereas *Myog* was exclusively methylated in the latter condition (Fig. 2D) (3). Remarkably, however, H2Bub was not detected on any of these genes in either state, despite extensive polymerase II (PolII) loading throughout each gene (3), consistent with its expression. We confirmed these observations by carrying out qChIP, which failed to detect H2Bub for all MRF genes over the entire differentiation time course, although each gene exhibited stage-specific, robust H3K4 trimethylation and, in some cases, H3K79me3 (Fig. 2D). Our analyses suggested that MRFs represent a group of genes that are never marked by detectable levels of H2Bub, regardless of their expression state.

The impact of RNF20 depletion on histone cross talk. The E3 ligase, RNF20, heterodimerizes with RNF40, and together, the complex acts as the major H2B ubiquitin ligase in mammalian cells (12, 22, 46). To determine whether RNF20 is responsible for ubiquitylation of H2B in myoblasts, we transiently and stably suppressed its expression with a unique siRNA and miRNA, respectively. Either treatment essentially abolished the expression of

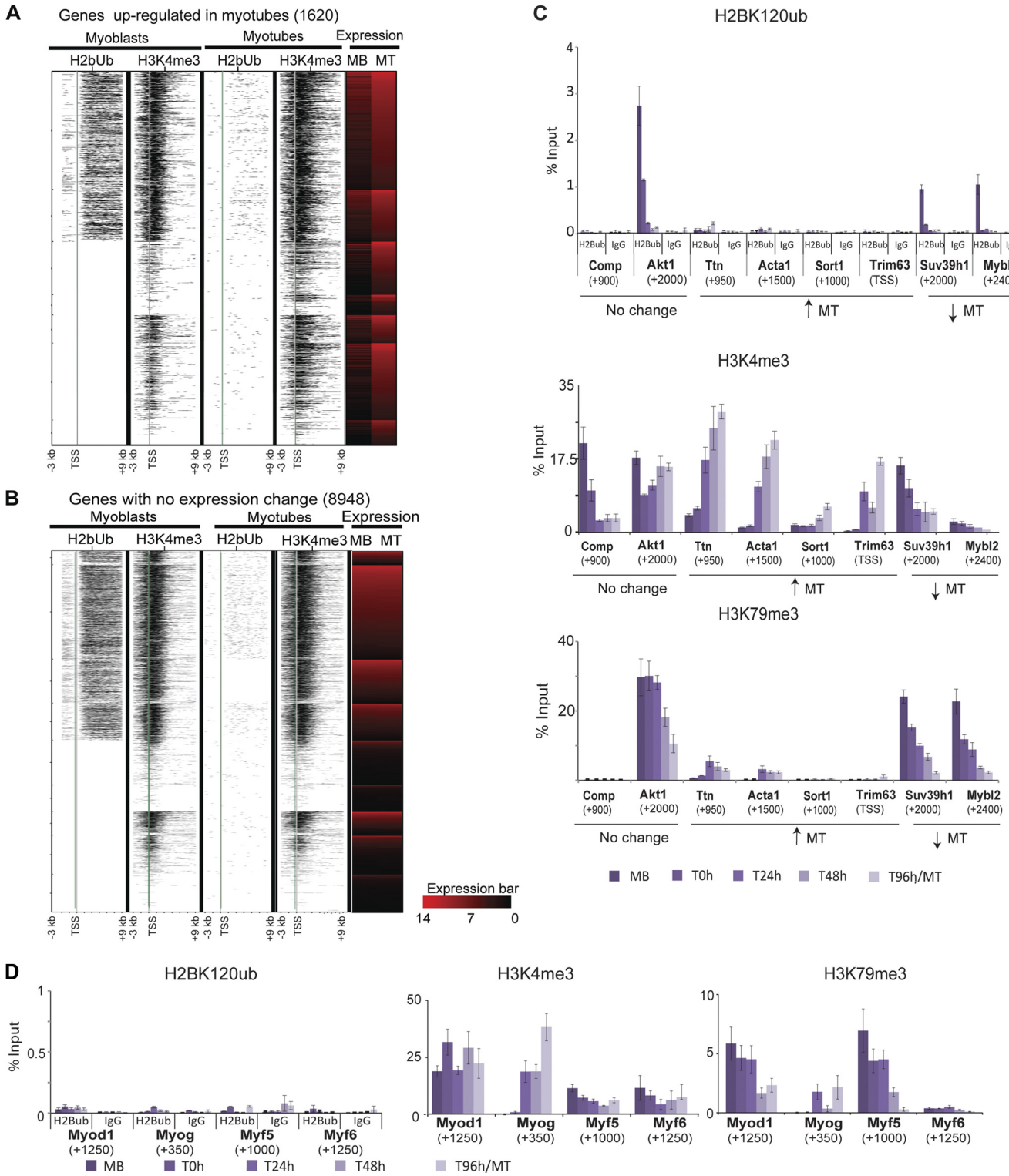

FIG 2 The relationship between H2Bub and H3K4 and H3K79 methylation in skeletal muscle. (A and B) High-density maps (HDMs) (Asp et al. [3]) for H2Bub and H3K4me3 in myoblasts and myotubes are shown. Horizontal rows represent individual genes, and the *x* axis represents the segment of each gene from −3 kb to +9 kb relative to the TSS (green vertical line). Expression levels are indicated as a red-black gradient (scale shown). A subset of the H3K4me3 data is depicted in Fig. 2 of Asp et al. (3). (C) ChIP was performed at indicated points during a myogenic differentiation time course to detect each histone modification. GM, growing myoblasts; T0h, T24h, and T48h, populations harvested 0, 24, and 48 h, respectively, after switching to differentiation medium; T96h/MT, fully differentiated myotubes. (D) Histone modifications were detected on genes encoding MRFs during myogenesis. All ChIP experiments were performed in triplicate, and error bars denote standard errors of the means.

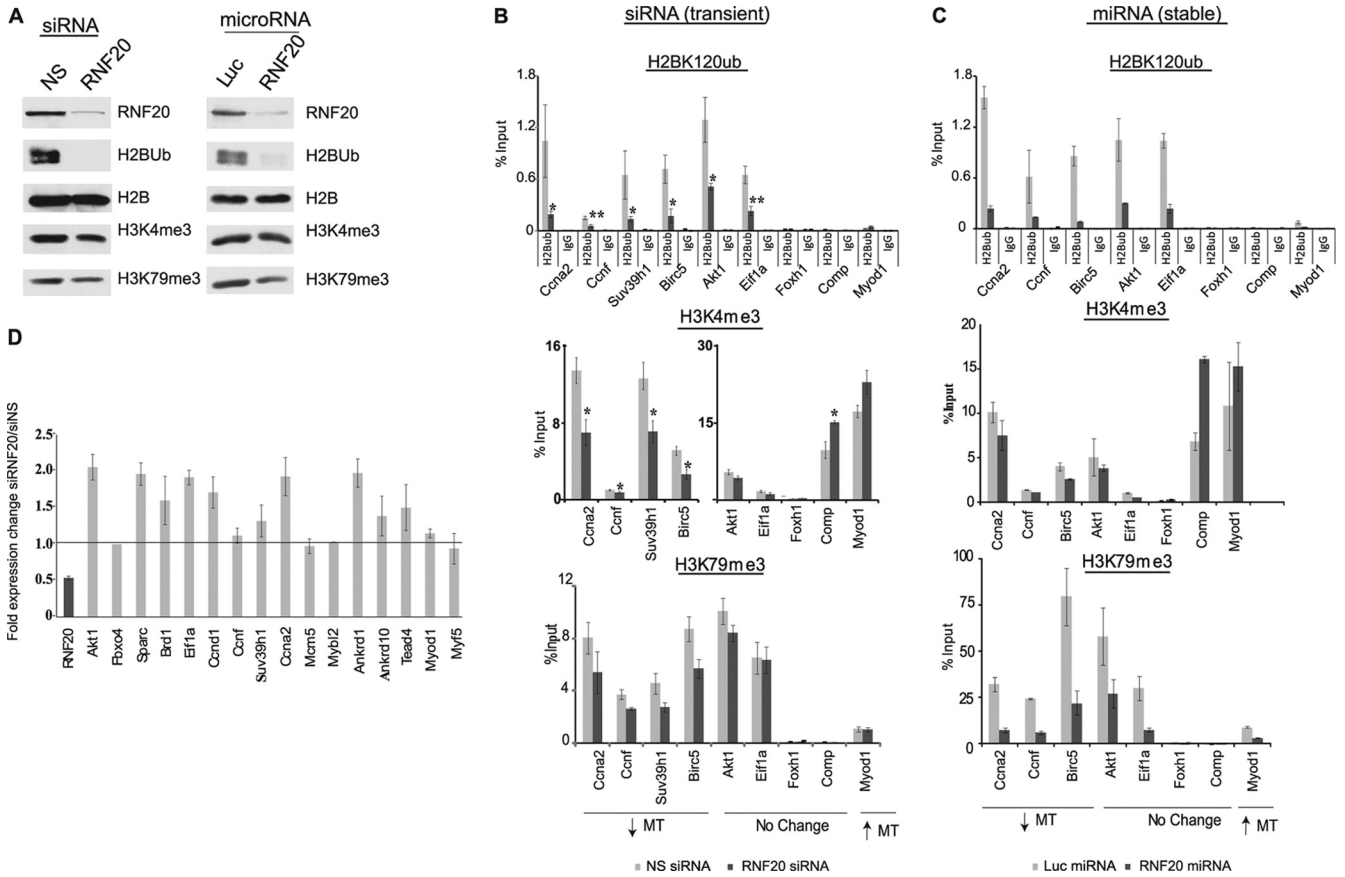

FIG 3 The impact of RNF20 suppression in muscle cells. (A) RNF20 expression was suppressed using an siRNA (left) and synthetic miRNA (right) in growing myoblasts, and Western blotting was performed to detect the indicated proteins. NS and Luc (luciferase), nonspecific controls. (B and C) ChIP was performed to detect the indicated histone marks after ablation of RNF20 with an siRNA (B) or miRNA (C). The ChIP results depicted are the averages of 3 to 6 independent experiments (B) or 2 independent experiments (C). The median positions of the amplicons as distances in bp from the TSS for the indicated genes are as follows: *Ccna2*, +2,000; *Ccnf*, +3,000; *Suv39h1*, +2,000; *Birc5*, +2,000; *Akt1*, +2,000; *Eif1a*, +2,000; *Foxh1*, +600; *Comp*, +900; and *Myod1*, +2,000. A Student *t* test was performed to calculate significance. *, $P < 0.05$; **, $P < 0.01$. (D) Quantitative RT-PCR was performed to detect changes in gene expression after RNF20 ablation. Fold change is expressed as the ratio of transcript levels in RNF20 siRNA- versus control-treated cells.

RNF20 and resulted in a sharp reduction in global H2Bub levels, confirming that RNF20 is the primary enzyme responsible for promoting this modification (Fig. 3A). In addition, we verified that RNF20 ablation substantially reduced H2Bub levels on several genes (Fig. 3B and C).

Ablating RNF20 and thereby reducing H2Bub levels allowed us to examine H3 methylation in myoblasts, a setting in which H2Bub levels are normally high and the two marks are expected to be coupled. RNF20 depletion led to modest decreases in overall H3K4me3 and H3K79me3 levels by Western analysis (Fig. 3A). Using qChIP, we examined H3 trimethylation on a representative group of genes that were constitutively expressed or downregulated during differentiation. On a subset of the latter group of genes (*Suv39h1*, *Birc5*, *Ccna2*, and *Ccnf*), the loss of H3K4me3 mirrored reductions in H2Bub, consistent with results in other mammalian systems (12, 42). However, on two constitutively expressed genes (*Eif1a* and *Akt1*), RNF20 depletion had little or no impact on H3K4me3 (Fig. 3B and C). Importantly, genes with little or no H2Bub in myoblasts (*Foxh1*, *Myod1*, and *Comp*) exhibited no difference or even modest increases in H3K4me3 when RNF20 was ablated, confirming that the observed results were direct and specific.

Interestingly, H3K79me3 levels showed modest changes resulting from transient siRNA-mediated suppression of RNF20. However, sustained miRNA-mediated depletion of RNF20 resulted in robust reductions in H3K79me3 levels (Fig. 3C), perhaps reflecting the stability of this mark. In addition, the levels of H3K79me3 closely paralleled those of H2Bub on these genes. These results favor the conclusion that H3K79me3 is tightly linked to H2Bub deposition. In contrast, long-term miRNA-mediated depletion resulted in only modest changes in H3K4me3, which resembled the results observed in our siRNA experiments (Fig. 3B).

Previous studies have suggested that changes in H3K4 trimethylation are due to altered gene expression induced by RNF20 suppression (35). We therefore examined the correlation between H3 methylation and gene expression after RNF20 depletion. RNF20 silencing had no effect on the expression of *Myod1* and *Myf5*, genes that are never marked by H2Bub. Importantly, certain genes exhibited elevated or unaltered expression in the face of reduced H3K4me3. *Ccnd1* and *Ccna2* were among a group of genes marked by H2Bub whose expression increased after RNF20 ablation (Fig. 3D), consistent with reports that H2Bub and RNF20 suppress the expression of genes involved in cell proliferation (34,

35). These results suggest that the observed reductions in H3K4me3 were not a result of decreased transcription but were more likely a direct result of reductions in H2Bub levels (Fig. 3B and C).

Thus, our combined studies of RNF20 ablation in myoblasts and normal myogenic differentiation reinforce the idea that levels of H2Bub and H3K4me3 are not always tightly correlated in either myoblasts or myotubes. This phenomenon is most pronounced in fully differentiated myotubes, wherein the expression of certain muscle-specific genes and H3K4 trimethylation appear to be largely independent of H2Bub. Although definitive evidence to rule out the absence of coupling of the two marks would require the complete ablation of factors required for H2B ubiquitylation (RNF20 and Rad6) in myotubes, technical challenges associated with RNAi in fully differentiated myotubes precluded these experiments. Thus, while it remains possible that transient, low levels of H2Bub (that are undetectable by ChIP) could promote H3K4me3 deposition in myotubes, our findings present a contrast to what is currently known regarding the correlation of these two marks in other systems. On the other hand, the deposition of H3K79me3 and H2Bub appear to be more tightly linked. Future studies are likely to reveal additional regulatory mechanisms that either buttress the cross talk between H2Bub and H3K4me3 or, alternatively, bypass the loss of H2Bub during myogenic differentiation.

Mechanisms associated with loss of H2Bub during differentiation. We next sought to determine the mechanistic basis for the loss of H2B ubiquitylation during myogenic differentiation and the apparent disconnect between H3K4me3 and H2Bub, and therefore, we examined the factors involved in depositing both modifications (Fig. 4A). In whole-cell lysates of C2C12 myoblasts and myotubes, the key ubiquitylation factors, RNF40 and Rad6, showed little or no change in levels before and after differentiation, although the RNF20 levels showed modest decreases during differentiation. In primary human myoblasts, we observed more dramatic decreases in RNF20, as well as Rad6, upon differentiation (Fig. 4A). Several components of the PAF complex (Paf1 and Cdc73) did not show significant changes in overall levels before and after differentiation, and the levels of the FACT subunit, Ssrp1, were somewhat reduced in myotubes compared to its levels in myoblasts, coinciding with reduced mRNA levels in expression profiling experiments (Fig. 4A). We also examined whether the assembly of H2B ubiquitylating complexes differed during myogenesis. Immunoprecipitations from nuclear extracts indicated that the level of association of RNF20 with RNF40 or Rad6 did not vary significantly as myoblasts differentiated into myotubes (Fig. 4B). Similarly, we did not observe overt changes in the integrity of Paf1C, since Leo1 readily coprecipitated with other Paf1C components in extracts from myoblasts and myotubes (Fig. 4B).

Next, we examined the extent to which factors relevant to H2B ubiquitylation are recruited to chromatin in myoblasts and myotubes. We used two methods to enrich for chromatin-bound proteins. First, we purified crude chromatin from formaldehyde-cross-linked myoblasts and myotubes using CsCl gradients (25, 27). This method enriches for proteins that are tightly associated with chromatin. Interestingly, RNF20 recruitment to chromatin was dramatically and reproducibly reduced in myotubes, although Rad6 levels remained unchanged (Fig. 4C, left). The FACT subunit, Ssrp1, showed a reduction in myotube versus myoblast chromatin, and Paf1 levels also showed modest reductions in myotube chromatin, although the differences were not as dramatic as that observed for RNF20. Likewise, we performed biochemical fractionation of soluble nuclear (S3 fraction) and chromatin-bound (P3 fraction) (Fig. 4C) proteins (21), which confirmed our observations regarding RNF20 (Fig. 4C, right). Interestingly, Rad6 partitioned to both compartments, and its recruitment to chromatin appeared to be considerably reduced in myotubes compared to that in myoblasts, perhaps reflecting technical differences in procedures used to obtain chromatin (Fig. 4C, compare left and right).

Since the association of RNF20 with chromatin diminished in myotubes, we investigated the recruitment of this factor to individual genes by performing qChIP (Fig. 4D). We observed enrichment of RNF20 on a subset of genes that were highly expressed in myoblasts, myotubes, or in both conditions. On genes that were highly expressed in myoblasts and myotubes, we observed significant RNF20 enrichment in myoblasts, but not in myotubes, consistent with our observation that H2Bub levels decrease markedly on these genes in myotubes (Fig. 4E). On genes that were highly induced in myotubes, RNF20 enrichment was comparable to background in both myoblasts and myotubes, in agreement with the fact that these genes do not show significant H2Bub enrichment in either condition, with the exception of *Acta1* (Fig. 4D and E). We also performed ChIP with antibodies against Rad6, but we were unable to detect convincing enrichment of this protein on any gene with two different antibodies (data not shown). We conclude that RNF20 is inefficiently recruited to chromatin in myotubes, providing a plausible mechanism for the reduction of H2Bub in myotubes.

Recruitment of transcriptional elongation factors Paf1C and FACT. Next, we explored the basis for the reduced RNF20 occupancy and low levels of H2Bub on genes that are highly expressed in myotubes by investigating the recruitment of specific elongation factors. Paf1C plays a role in transcriptional elongation and modification of histones. First, it is thought to assist in recruiting the COMPASS complex, facilitating H3K4 methylation in yeast (14, 15). Paf1C also interacts with RNF20 and Rad6, stimulating H2B ubiquitylation activity in transcribed regions of active genes and thereby promoting H3K4 trimethylation (13, 15). We investigated the recruitment of Paf1C to genes exhibiting H3K4me3 using antibodies against Paf1 (Fig. 4F). We made several notable observations. First, on genes that were highly expressed in myoblasts and myotubes (e.g., *Ran* and *Lgals1*), the pattern of reduced Paf1 recruitment mirrored that of RNF20, potentially accounting for the loss of RNF20 on these genes in myotubes (Fig. 4D and F). However, on genes that were markedly upregulated in myotubes without detectable H2Bub (e.g., *Myh3*, *Trim63*, and *Myog*), significant Paf1 recruitment was detected *de novo* in myotubes, in stark contrast with the pattern observed for RNF20, reinforcing the idea that Paf1C could play a role in events beyond recruitment of H2B ubiquitylating factors.

We also investigated the recruitment of FACT to the same group of genes by performing qChIP with antibodies against Ssrp1. FACT positively regulates transcriptional elongation by modulating nucleosome dynamics (45). FACT is also thought to act synergistically with Paf1C and H2B ubiquitylation for efficient transcription of *in vitro* reconstituted, chromatinized templates (28). Our results indicate that FACT recruitment coincides with expression in myoblasts and myotubes (Fig. 4G), since we observed robust enrichment of FACT on genes (e.g., *Lgals1* and *Ran*) that were highly expressed in both conditions. Significant FACT

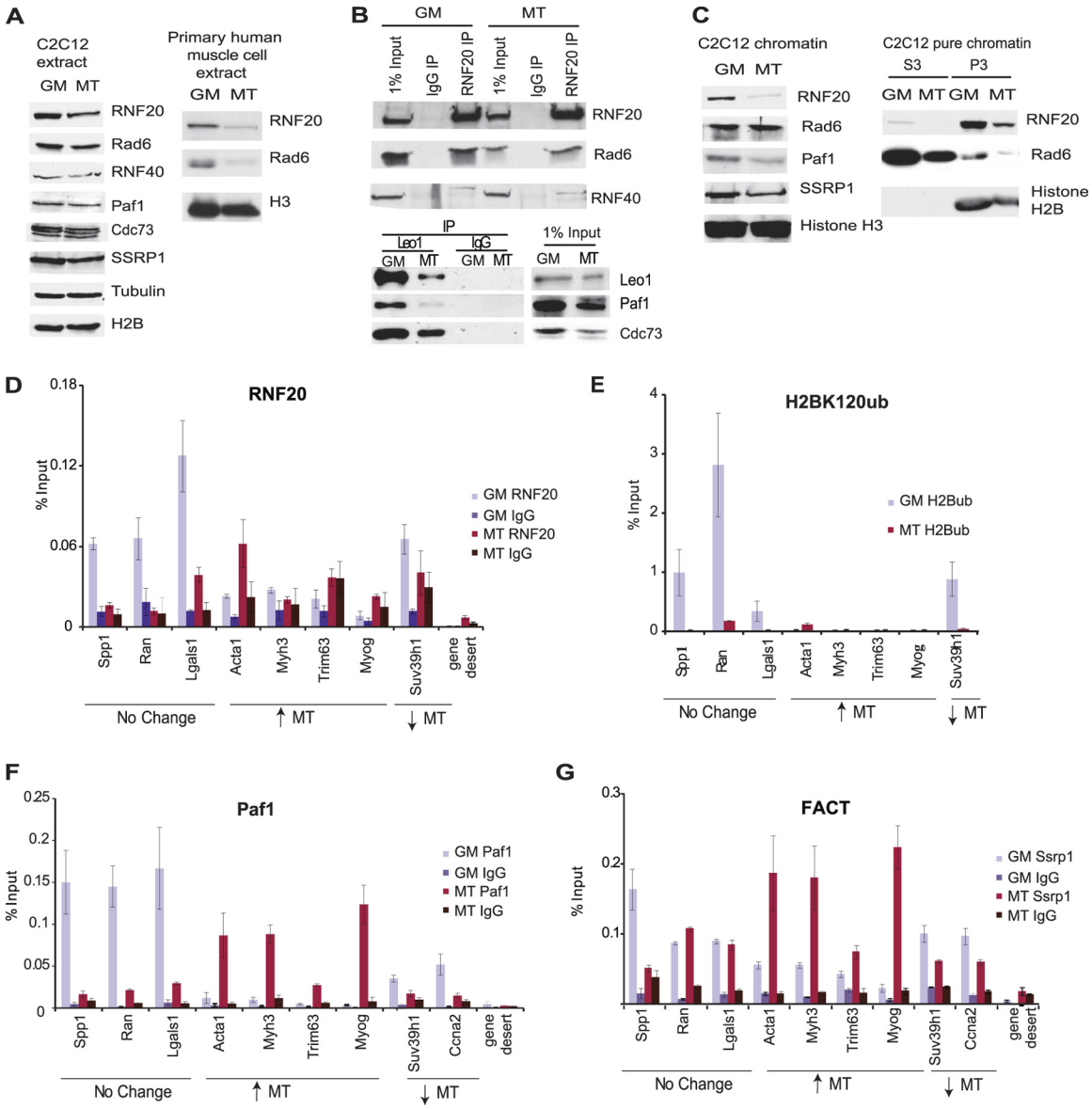

FIG 4 Mechanistic explanation for loss of H2Bub in myotubes. (A) Western analysis to detect expression of ubiquitylation and elongation factors in myoblast and myotube whole-cell extracts from C2C12 (left) and primary human skeletal muscle (right) cells. (B) RNF20 was immunoprecipitated from nuclear extracts, and RNF20, RNF40, and Rad6 were detected as indicated. IgG IP, negative control. (C) Chromatin was purified using centrifugation through CsCl gradients (left) or by fractionation into soluble nuclear (S3) and chromatin (P3) compartments (right). (D to G) ChIP was performed to detect the indicated histone modifications (H2Bub) and factors (RNF20, Ssrp1/FACT, and Paf1). The median positions of the amplicons as distances in bp from the TSS for the indicated genes are as follows: *Spp1*, +1,000; *Ran*, +1,500; *Lgals1*, +50; *Acta1*, +1,200; *Myh3*, +6,500; *Trim63*, TSS; *Myog*, +350; *Ccna2*, +2,000; and *Suv39h1*, +2,000. Enrichment is indicated as a function of percent input on the *y* axis.

enrichment was also observed on genes (*Acta1*, *Myog*, *Trim63*, and *Myh3*) that were upregulated in myotubes, mimicking Paf1 recruitment (Fig. 4G). Taken together, these data suggest that the absence of H2B ubiquitylation does not have a bearing on either Paf1C or FACT recruitment in myotubes. Furthermore, recruitment of these factors does not appear to presage H2B ubiquitylation, in contrast with previous observations relating FACT and Paf1C to this modification, and this is most evident on genes that are upregulated in myotubes. Future studies involving detailed analyses of other factors that function in RNF20 recruitment, such as WAC (44), may provide additional insight into the mechanisms underlying the loss of RNF20 from myotube chromatin.

Recruitment of Wdr82 in myotubes occurs independently of H2Bub. We next examined factors responsible for depositing the H3K4me3 mark. In mammals, H3K4 trimethylation is catalyzed by several different H3K4 methylase-containing complexes, including MLL (1, 2, 3, and 4), Set1A, and Set1B, whereas a single complex (COMPASS) performs this function in yeast. MLL and Set1 complexes share a number of common subunits, but they can be differentiated biochemically by examining unique components. Further, MLL and Set1A/B complexes may perform nonredundant functions by regulating different groups of genes and by modulating distinct steps in the transcription cycle. It is thought that the Set1A and Set1B complexes more closely resemble

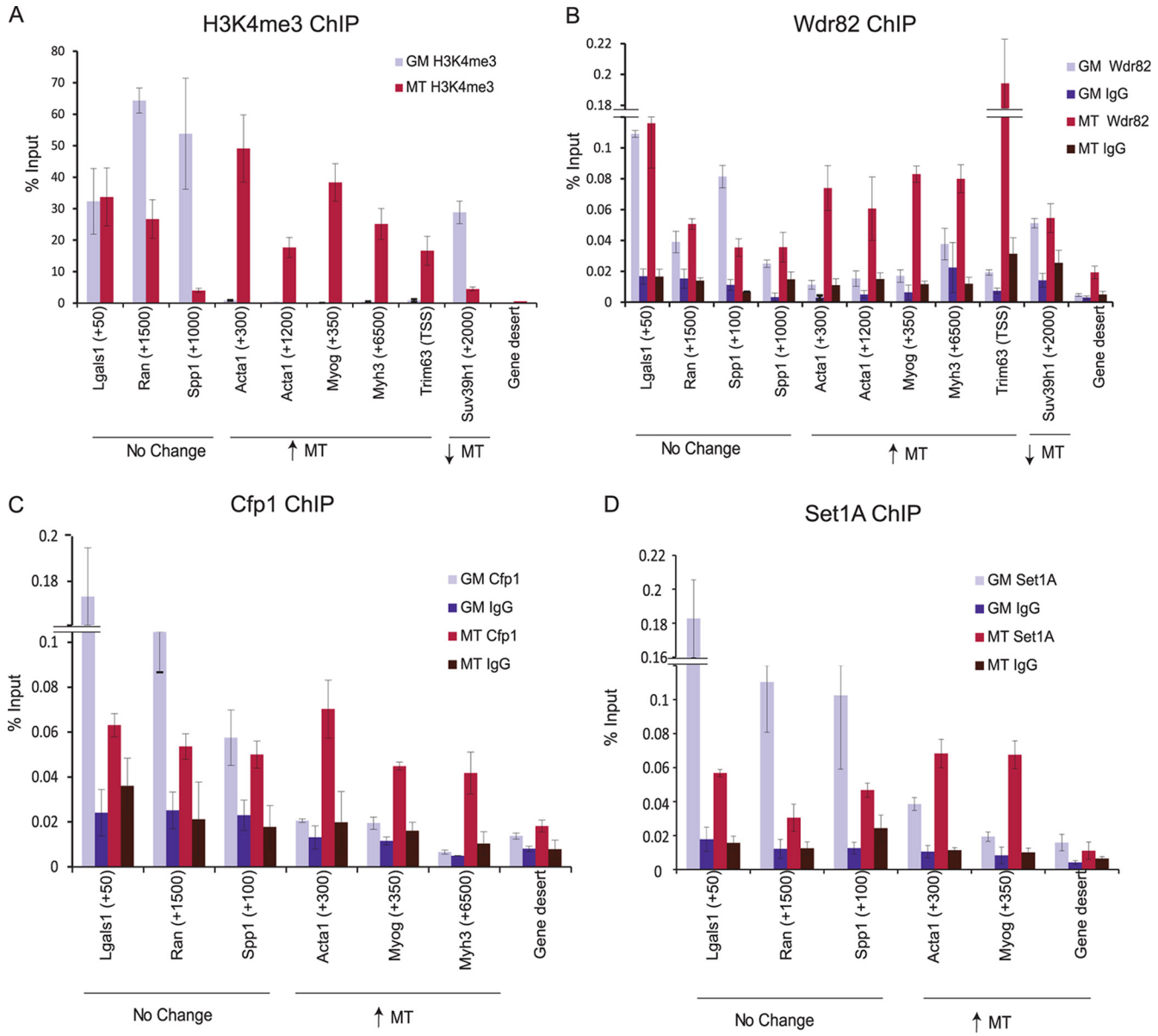

FIG 5 Recruitment of Wdr82 and the Set1 complex in myotubes is independent of H2B ubiquitylation and correlates with H3K4me3. (A) qChIP was performed to detect H3K4me3 on the indicated genes. (B to D) qChIP was performed in myoblasts (GM) and myotubes (MT) to detect factors (Wdr82, Set1A, and Cfp1) on the indicated genes, and nonspecific rabbit IgG and an amplicon in a gene desert were used as controls in each case. Enrichment is indicated as a function of percent input on the *y* axis.

COMPASS, since the unique mammalian components of this complex, Wdr82 and Cfp1, are homologous to Cps35 and Cps40 in the yeast complex (16). Recruitment of the Set1A/B complex to chromatin is thought to be dependent on H2B ubiquitylation, enabling it to function subsequent to transcriptional initiation. Indeed, both yeast and mammalian studies have shown that H3K4 trimethylation is modulated through the H2Bub-dependent recruitment of the Cps35/Wdr82 component of the Set1/COMPASS complex (19, 42, 45). In contrast, MLL complexes lack Wdr82 and have been implicated in regulating *Hox* gene function at the level of gene activation (40), suggesting that MLL-mediated H3K4 methylation may be independent of H2B ubiquitylation (36). In addition, experiments with MLL knockout mice indicate that MLLs may regulate H3K4 methylation on a subset of genes (40), whereas the Set1A/B complex may represent the major H3K4 trimethylase in mammalian cells, since depletion of either Wdr82 or RNF20 has been shown to reduce overall H3K4 trimethylation levels (16, 42).

Having observed robust H3K4 trimethylation in the absence of H2Bub, we investigated the methylases that were responsible for depositing the former mark in myotubes by performing ChIP with antibodies against components of the Set1 and MLL complexes in myoblasts and myotubes. First, we observed enrichment of Wdr82 on several genes that were highly expressed in myoblasts, myotubes, or both (Fig. 5B). The levels of Wdr82 enrichment coincided with that of H3K4me3 and correlated with the expression of

genes in myoblasts as well as myotubes (Fig. 5A and B). Genes marked with H3K4me3 in myoblasts and myotubes (*Lgals1* and *Ran*) showed significant Wdr82 enrichment in both conditions. In contrast, genes that were markedly induced in myotubes exhibited concomitant increases in H3K4me3 levels (e.g., *Myh3*, *Trim63*, and *Myog*) and robust recruitment of Wdr82 in myotubes only. This was unanticipated given the lack of detectable H2Bub deposition on these genes in either condition (Fig. 4E).

Since the overall levels of enrichment were relatively low, we performed controls to verify the specificity of this antibody. We found that siRNA-mediated knockdown of Wdr82 led to drastic reductions in recruitment of this protein to chromatin, as expected (data not shown). Since Wdr82 is thought to associate with other complexes in yeast and in humans (18, 23), we further examined whether additional Set1 complex components, Set1A and Cfp1, were similarly recruited to Wdr82 target genes. Indeed, these components were detected on a number of target genes (Fig. 5C and D). Importantly, we also observed recruitment of these components in myotubes. Taken together, these data suggest that Set1 complexes can be recruited to genes without detectable H2Bub in myotubes, although deposition of this modification is thought to precede recruitment of Wdr82 and the formation of active trimethylase complexes on chromatin.

Our experiments did not address the possibility that other H3K4 methylase complexes, namely, MLLs, could also be involved in implementing H3K4 trimethylation in myotubes, since their recruitment is thought to be independent of H2B ubiquitylation. Therefore, we investigated whether the target genes in our study recruited MLLs 1 and 2 using ChIP with antibodies against menin, a protein common to both MLL complexes (data not shown). Of note, menin was not detected on several muscle-specific genes that are enriched for H3K4me3 in myotubes, although this protein was recruited to the *Hoxa9* promoter, as expected from studies in other mammalian cells (40). It is possible that other MLL complexes (MLL3/4) could be recruited to the genes we have examined, but the lack of available antibodies able to detect these proteins in ChIP experiments precluded us from testing their recruitment to chromatin. Our data, therefore, do not rule out the role of MLLs in contributing to H3K4 trimethylation of genes in myotubes.

Set1 complexes exhibit methyltransferase activity on target genes. Next, we tested whether the Set1 complex could function as an active methyltransferase on genes to which it was recruited. Upon carrying out siRNA-mediated knockdown of Wdr82 in myoblasts, we observed a global loss of H3K4me3, similar to what has been observed in other mammalian cell types (Fig. 6A) (16, 42). Importantly, we also observed a reproducible and significant reduction in H3K4me3 on genes that recruited Wdr82 (Fig. 6B), together with a reduction in Set1A recruitment to these genes (data not shown). These data indicate that Set1 complexes (that contain Wdr82) represent a major H3K4me3 methylase on these genes in C2C12 cells. Although Wdr82 knockdown in fully differentiated myotubes was somewhat less efficient owing to technical challenges associated with transfection of siRNAs in fully differentiated myotubes, the expression of Wdr82 protein was reduced ~50%, and H3K4me3 was also reduced on several target genes (data not shown). Thus, since three components of the Set1 complex (Set1A, Wdr82, and Cfp1) were recruited to genes in a manner that coincided with the acquisition of H3K4me3 in myoblasts and myotubes, we conclude that the Set1 complex promotes this modification on these genes in both conditions.

Taken together, our data indicate that the Set1/COMPASS complex plays an important role in establishing H3K4 methylation in C2C12 cells, and the recruitment of this complex to an array of genes that we have examined appears to be largely independent of detectable H2B ubiquitylation during myogenic differentiation. However, in order to generalize our findings regarding the relative contributions of Set1 and the MLL complexes, it will be essential to perform more extensive, genome-wide experiments. For example, once reagents able to detect all MLL complexes are available, it will be possible to more comprehensively define the occupancy of all H3K4 trimethylases on genes that exhibit H3K4me3 in the absence of H2Bub in myotubes.

Concluding remarks. Over the past decade, many studies have shed light on mechanisms that couple the deposition of multiple histone modifications. However, recent experiments, including our studies in muscle cells, suggest that our understanding is far from complete. For example, although a tight connection between H2Bub and trimethylation of H3K4 and H3K79 has been established in yeast, it is not an obligatory event in *Tetrahymena thermophila* (41). Interestingly, *Tetrahymena* does not possess Set1/COMPASS type methylases and instead expresses a single methylase closely related to MLL (36, 41), which could offer a possible explanation for the loss of H2Bub dependence. In mammalian systems, the presence of several different methylase complexes, some of which have H2Bub-independent functions, make the connection between H2B ubiquitylation and H3K4 methylation more complex. Thus, the coupling mechanisms and the contributions from distinct methylases could vary according to cell type and, perhaps, growth conditions. Our results indicate that the Set1 complex deposits H3K4 trimethylation at several genes despite the global loss of H2Bub in myotubes. These observations suggest alternative mechanisms by which Set1 could be recruited to genes, through as yet unknown protein-DNA and protein-protein interactions. Moreover, additional experiments will be required to comprehensively test the role of MLL complexes during myogenesis, once suitable reagents able to detect all four MLL complexes have been developed, particularly in light of our finding that H3K4me3 levels do not globally change in a commensurate way during myogenesis (3).

Further studies will be required to obtain a complete understanding of the regulatory mechanisms that underlie transcriptional elongation and nucleosome dynamics during myogenic differentiation. It is likely that the role of H2Bub in gene expression will be more complex than anticipated (4, 10, 28, 34). For example, a number of studies have shown that H2Bub plays a modulatory role in transcription through its control of elongation and nucleosome dynamics, in a manner that is distinct from its functions in histone cross talk. Thus, it is clear that H2Bub could have roles that are independent of H3 methylation and that the bulk of H2Bub (as detected by our assays) could regulate other aspects of gene expression. It is also interesting to speculate that certain populations of H2Bub, such as those that promote H3K4me3 in muscle cells, are more transiently associated with chromatin than others, and such a scenario has been observed in yeast (4, 31).

Several interesting questions arise as to how cells could bypass a requirement for detectable levels of H2Bub in the regulation of gene expression and chromatin dynamics. Myogenic differentiation is also accompanied by other large-scale epigenetic changes

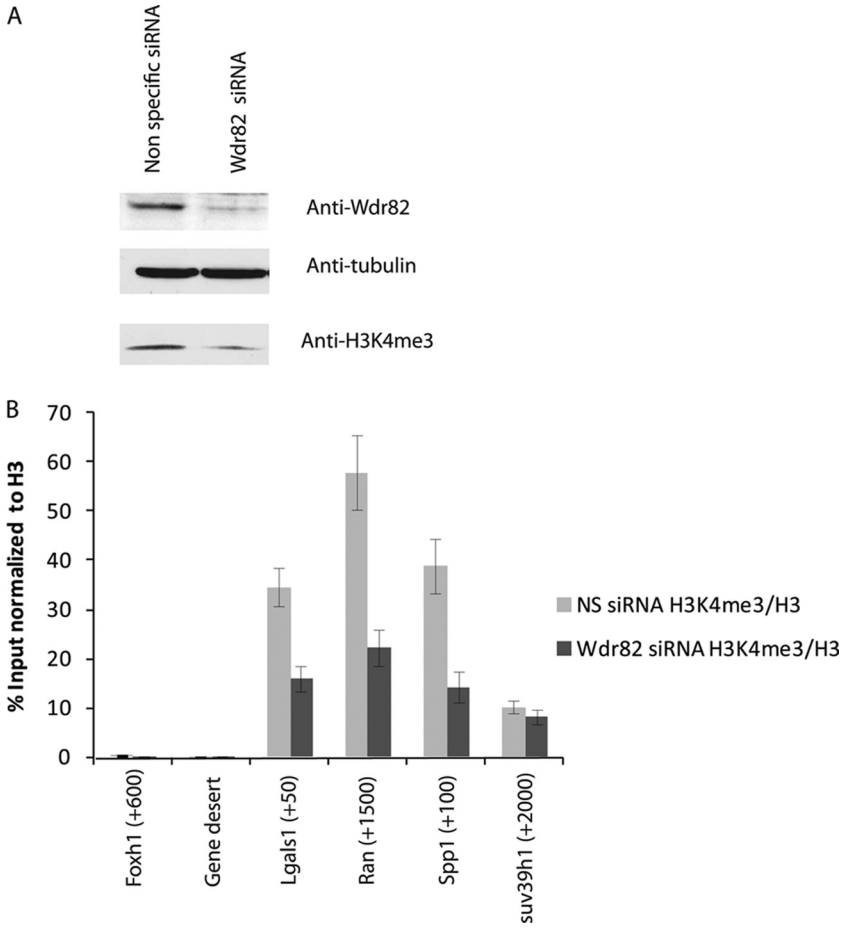

FIG 6 Set1 complexes recruited to genes exhibit methyltransferase activity. (A) Western blotting was performed to detect the suppression of Wdr82 protein and H3K4me3 levels upon transfecting siRNAs targeting Wdr82 compared to the results using a control siRNA (NS [nonspecific]). Tubulin was used as a loading control. (B) qChIP was performed to detect the diminution of H3K4me3 on genes upon Wdr82 knockdown in myoblasts. Simultaneously, qChIP was performed with anti-H3 antibodies, and enrichment is shown as a function of percent input by presenting the ratio of H3K4me3/H3 on the *y* axis.

(3), including overall deacetylation. Since acetylation has a potentially destabilizing effect on nucleosome formation, it is possible that H2Bub may not be essential for nucleosome stability in the face of diminished levels of acetylation. Alternatively, other as-yet-unknown epigenetic changes accompanying myogenic differentiation may preclude the need for H2Bub in modulating nucleosome dynamics and gene expression. It will be interesting to determine whether our observations are relevant to other developmental settings and diverse types of terminal differentiation. We propose that muscle cells represent an interesting system in which to explore these questions, and future studies will focus on a broader role played by H2Bub in the context of cell type specification and differentiation.

ACKNOWLEDGMENTS

We are most grateful to D. Reinberg for the gift of antibodies. We thank the members of the Dynlacht laboratory for constructive advice and the NYU Genome Technology Center for Illumina sequencing. We thank F. Parisi, M. Micsinai, and Y. Kluger for developing Qeseq and for computational assistance in generating HDMs (Fig. 2). We thank R. Blum for computational assistance and helpful advice.

V. Vethantham was supported initially by an NIH training grant and is currently supported by an American Cancer Society postdoctoral fellowship (PF-11-043-01-DMC). Brian D. Dynlacht was supported by NIH grants R01GM067132 and 5R01CA077245. The Wdr82, Set1A, and Cfp1 antisera were produced with the support of the NSF (grant MCB-0641851).

REFERENCES

1. **Acosta-Alvear D, et al.** 2007. XBP1 controls diverse cell type- and condition-specific transcriptional regulatory networks. Mol. Cell **27**: 53–66.
2. **Asp P, Acosta-Alvear D, Tsikitis M, van Oevelen C, Dynlacht BD.** 2009. E2f3b plays an essential role in myogenic differentiation through isoform-specific gene regulation. Genes Dev. **23**:37–53.
3. **Asp P, et al.** 2011. Genome-wide remodeling of the epigenetic landscape during myogenic differentiation. Proc. Natl. Acad. Sci. U. S. A. **108**:E149–E158.
4. **Batta K, Zhang Z, Yen K, Goffman DB, Pugh BF.** 2011. Genome-wide function of H2B ubiquitylation in promoter and genic regions. Genes Dev. **25**:2254–2265.
5. **Blais A, van Oevelen CJ, Margueron R, Acosta-Alvear D, Dynlacht BD.** 2007. Retinoblastoma tumor suppressor protein-dependent methylation of histone H3 lysine 27 is associated with irreversible cell cycle exit. J. Biol. Chem. **179**:1399–1412.
6. **Briggs SD, et al.** 2002. Gene silencing: trans-histone regulatory pathway in chromatin. Nature **418**:498.
7. **Dehe PM, et al.** 2005. Histone H3 lysine 4 mono-methylation does not require ubiquitination of histone H2B. J. Mol. Biol. **353**:477–484.

8. **Dover J, et al.** 2002. Methylation of histone H3 by COMPASS requires ubiquitination of histone H2B by Rad6. J. Biol. Chem. **277**:28368–28371.
9. **Fierz B, et al.** 2011. Histone H2B ubiquitylation disrupts local and higher-order chromatin compaction. Nat. Chem. Biol. **7**:113–119.
10. **Fleming AB, Kao CF, Hillyer C, Pikaart M, Osley MA.** 2008. H2B ubiquitylation plays a role in nucleosome dynamics during transcription elongation. Mol. Cell **31**:57–66.
11. **Hwang WW, et al.** 2003. A conserved RING finger protein required for histone H2B monoubiquitination and cell size control. Mol. Cell **11**:261–266.
12. **Kim J, et al.** 2009. RAD6-mediated transcription-coupled H2B ubiquitylation directly stimulates H3K4 methylation in human cells. Cell **137**:459–471.
13. **Kim J, Roeder RG.** 2009. Direct Bre1-Paf1 complex interactions and RING finger-independent Bre1-Rad6 interactions mediate histone H2B ubiquitylation in yeast. J. Biol. Chem. **284**:20582–20592.
14. **Krogan NJ, et al.** 2003. The Paf1 complex is required for histone H3 methylation by COMPASS and Dot1p: linking transcriptional elongation to histone methylation. Mol. Cell **11**:721–729.
15. **Laribee RN, et al.** 2005. BUR kinase selectively regulates H3 K4 trimethylation and H2B ubiquitylation through recruitment of the PAF elongation complex. Curr. Biol. **15**:1487–1493.
16. **Lee JH, Skalnik DG.** 2008. Wdr82 is a C-terminal domain-binding protein that recruits the Setd1A histone H3-Lys4 methyltransferase complex to transcription start sites of transcribed human genes. Mol. Cell. Biol. **28**:609–618.
17. **Lee JH, Tate CM, You JS, Skalnik DG.** 2007. Identification and characterization of the human Set1B histone H3-Lys4 methyltransferase complex. J. Biol. Chem. **282**:13419–13428.
18. **Lee JH, You J, Dobrota E, Skalnik DG.** 2010. Identification and characterization of a novel human PP1 phosphatase complex. J. Biol. Chem. **285**:24466–24476.
19. **Lee JS, et al.** 2007. Histone crosstalk between H2B monoubiquitination and H3 methylation mediated by COMPASS. Cell **131**:1084–1096.
20. **McGinty RK, Kim J, Chatterjee C, Roeder RG, Muir TW.** 2008. Chemically ubiquitylated histone H2B stimulates hDot1L-mediated intranucleosomal methylation. Nature **453**:812–816.
21. **Mendez J, Stillman B.** 2000. Chromatin association of human origin recognition complex, cdc6, and minichromosome maintenance proteins during the cell cycle: assembly of prereplication complexes in late mitosis. Mol. Cell. Biol. **20**:8602–8612.
22. **Minsky N, et al.** 2008. Monoubiquitinated H2B is associated with the transcribed region of highly expressed genes in human cells. Nat. Cell Biol. **10**:483–488.
23. **Nedea E, et al.** 2008. The Glc7 phosphatase subunit of the cleavage and polyadenylation factor is essential for transcription termination on snoRNA genes. Mol. Cell **29**:577–587.
24. **Ng HH, Xu RM, Zhang Y, Struhl K.** 2002. Ubiquitination of histone H2B by Rad6 is required for efficient Dot1-mediated methylation of histone H3 lysine 79. J. Biol. Chem. **277**:34655–34657.
25. **Orlando V, Strutt H, Paro R.** 1997. Analysis of chromatin structure by in vivo formaldehyde cross-linking. Methods **11**:205–214.
26. **Orphanides G, LeRoy G, Chang CH, Luse DS, Reinberg D.** 1998. FACT, a factor that facilitates transcript elongation through nucleosomes. Cell **92**:105–116.
27. **Parekh BS, Maniatis T.** 1999. Virus infection leads to localized hyperacetylation of histones H3 and H4 at the IFN-beta promoter. Mol. Cell **3**:125–129.
28. **Pavri R, et al.** 2006. Histone H2B monoubiquitination functions cooperatively with FACT to regulate elongation by RNA polymerase II. Cell **125**:703–717.
29. **Pirngruber J, et al.** 2009. CDK9 directs H2B monoubiquitination and controls replication-dependent histone mRNA 3′-end processing. EMBO Rep. **10**:894–900.
30. **Robzyk K, Recht J, Osley MA.** 2000. Rad6-dependent ubiquitination of histone H2B in yeast. Science **287**:501–504.
31. **Schulze JM, et al.** 2011. Splitting the task: Ubp8 and Ubp10 deubiquitinate different cellular pools of H2BK123. Genes Dev. **25**:2242–2247.
32. **Schwabish MA, Struhl K.** 2004. Evidence for eviction and rapid deposition of histones upon transcriptional elongation by RNA polymerase II. Mol. Cell. Biol. **24**:10111–10117.
33. **Shahbazian MD, Zhang K, Grunstein M.** 2005. Histone H2B ubiquitylation controls processive methylation but not monomethylation by Dot1 and Set1. Mol. Cell **19**:271–277.
34. **Shema E, Kim J, Roeder RG, Oren M.** 2011. RNF20 inhibits TFIIS-facilitated transcriptional elongation to suppress pro-oncogenic gene expression. Mol. Cell **42**:477–488.
35. **Shema E, et al.** 2008. The histone H2B-specific ubiquitin ligase RNF20/hBRE1 acts as a putative tumor suppressor through selective regulation of gene expression. Genes Dev. **22**:2664–2676.
36. **Smith E, Lin C, Shilatifard A.** 2011. The super elongation complex (SEC) and MLL in development and disease. Genes Dev. **25**:661–672.
37. **Sun ZW, Allis CD.** 2002. Ubiquitination of histone H2B regulates H3 methylation and gene silencing in yeast. Nature **418**:104–108.
38. **Tanny JC, Erdjument-Bromage H, Tempst P, Allis CD.** 2007. Ubiquitylation of histone H2B controls RNA polymerase II transcription elongation independently of histone H3 methylation. Genes Dev. **21**:835–847.
39. **van Oevelen C, et al.** 2008. A role for mammalian Sin3 in permanent gene silencing. Mol. Cell **32**:359–370.
40. **Wang P, et al.** 2009. Global analysis of H3K4 methylation defines MLL family member targets and points to a role for MLL1-mediated H3K4 methylation in the regulation of transcriptional initiation by RNA polymerase II. Mol. Cell. Biol. **29**:6074–6085.
41. **Wang Z, Cui B, Gorovsky MA.** 2009. Histone H2B ubiquitylation is not required for histone H3 methylation at lysine 4 in tetrahymena. J. Biol. Chem. **284**:34870–34879.
42. **Wu M, et al.** 2008. Molecular regulation of H3K4 trimethylation by Wdr82, a component of human Set1/COMPASS. Mol. Cell. Biol. **28**:7337–7344.
43. **Xiao T, et al.** 2005. Histone H2B ubiquitylation is associated with elongating RNA polymerase II. Mol. Cell. Biol. **25**:637–651.
44. **Zhang F, Yu X.** 2011. WAC, a functional partner of RNF20/40, regulates histone H2B ubiquitination and gene transcription. Mol. Cell **41**:384–397.
45. **Zheng S, Wyrick JJ, Reese JC.** 2010. Novel trans-tail regulation of H2B ubiquitylation and H3K4 methylation by the N terminus of histone H2A. Mol. Cell. Biol. **30**:3635–3645.
46. **Zhu B, et al.** 2005. Monoubiquitination of human histone H2B: the factors involved and their roles in HOX gene regulation. Mol. Cell **20**:601–611.